A structural insight into the inhibition of human and Leishmania donovani ornithine decarboxylases by 1-amino-oxy-3-aminopropane

Veronica Tamu Dufe, Daniel Ingner, Olle Heby, Alex R Khomutov, Lo Persson, Salam Al-Karadaghi

Biochemical Journal Immediate Publication. Published on 4 Apr 2007 as manuscript BJ20070188

A structural insight into the inhibition of human and *Leishmania donovani* ornithine decarboxylases by 3-aminooxy-1-aminopropane

Veronica Tamu Dufe*, Daniel Ingner*, Olle Heby[†], Alex R. Khomutov[‡], Lo Persson[§ 1] & Salam Al-Karadaghi* [1].

Departments of [*]Molecular Biophysics and [§]Experimental Medical Science, Lund University, S-221 00 and S-221 84 Lund, Sweden.

[†] Department of Molecular Biology, Umeå University, S-901 87 Umeå, Sweden.

[‡] Engelhardt Institute of Molecular Biology, Russian Academy of Sciences, Moscow, 119991 Russia

[1]) Corresponding authors:

Salam Al-Karadaghi,
Departments of Molecular Biophysics, Center for Chemistry and Chemical Engineering, Lund University, P.O. Box 124, S-221 00 Lund, Sweden.
e-mail: salam.al-karadaghi@mbfys.lu.se
Tel. +46(0)462224512, Fax. +46(0)462224692

Lo Persson
Department of Experimental Medical Science, Lund University, S-221 84 Lund, Sweden.
e-mail: Lo.Persson@med.lu.se
Tel: 046-2227746, Fax: 046-2224546

ABSTRACT

The critical role of polyamines in key processes like cell growth, differentiation and macromolecular synthesis makes the enzymes involved in their synthesis potential targets in the treatment of certain types of cancer and parasitic diseases. Here we present a study on the inhibition of human and *Leishmania donovani* ornithine decarboxylase (ODC), the first committed enzyme in the polyamine biosynthesis pathway, by 1-aminooxy-3-aminopropane (APA). The study shows APA to be a potent inhibitor of both human and *L. donovani* ODC with a Ki value of around 1.0 nM. We also show that *L. donovani* ODC binds the substrate, the coenzyme pyridoxal 5'-phosphate and the irreversible inhibitor α-difluoromethylornithine (a curative agent of West African sleeping sickness) with less affinity than human ODC. We have also determined the three-dimensional structure of human ODC in complex with APA, which revealed the mode of the inhibitor binding to the enzyme. In contrast to earlier suggestions, the structure showed no indication of oxime formation between APA and pyridoxal 5'-phosphate. Homology modelling suggests a similar mode of binding of APA to *L. donovani* ODC. A comparison of the ODC-APA-PLP structure with earlier ODC structures also shows that the protease sensitive-loop (residues 158-168) undergoes a large conformational change and covers the active site of the protein. The understanding of the structural mode of APA binding may constitute the basis for the development of more specific inhibitors of *L. donovani* ODC.

Short title: Structure of APA complex of ornithine decarboxylase

Key words: polyamine synthesis, drug target, tropical parasites, cancer, inhibitor complex

Abbreviations: ODC - ornithine decarboxylase; PLP - pyridoxal 5′-phosphate; DFMO - α-difluoromethylornithine; APA - 3-aminooxy-1-aminopropane

Introduction

The first and rate-limiting step in the polyamine biosynthetic pathway is the conversion of ornithine to putrescine. This reaction is catalyzed by ornithine decarboxylase (ODC), a pyridoxal 5´-phosphate (PLP, vitamin B_6)-dependent enzyme, known to form obligate dimers in eukaryotes [1]. The critical role of polyamines in key processes like cell growth, differentiation and macromolecular synthesis makes the enzymes involved in their synthesis potential targets in the treatment of certain types of cancer [2;3] and parasitic diseases [4-6]. Thus, the irreversible ODC inhibitor, α-difluoromethylornithine (DFMO) is currently used for the treatment of patients with advanced West African sleeping sickness, caused by the protozoan parasite *Trypanosoma brucei gambiense* [6;7] DFMO also exhibits some activity against other parasitic protozoa, like *Plasmodium falciparum, P. berghei* [8] and *L. donovani* [9]. Another compound, 3-aminooxy-1-aminopropane (APA), an isosteric analog of putrescine, is a more potent inhibitor of ODC with inhibition constants in the nM range [10;11]. APA and its derivatives exert antiproliferative effects on various tumor cells and parasites [12-17]. Similar to other aminooxy analogues, the inhibition of ODC by APA has been suggested to proceed through the formation of an oxime with PLP in the enzyme's active site [10;18;19].

The X-ray structures of ODC from mouse [20], *T. brucei* [21;22] and human [23], show a dimeric enzyme in which each N-terminal domain is a TIM-like α/β-barrel and each C-terminal domain forms a β-sheet. The two active sites are found at the dimer interface, between the N-terminal domain of one monomer and the C-terminal domain of the other, with Lys-69 and Cys-360 contributing to each active site from opposite monomers [24;25]. The structures also identified the residues important for PLP binding and interactions with DFMO [21;26]. In this work we present the kinetic parameters of inhibition of human and *L. donovani* ODC by APA, as well as the crystal structure of the complex between APA and human ODC. The structure shows that APA is bound in the substrate binding pocket in close proximity to PLP. However, no oxime formation is observed between the inhibitor and PLP. Examination of the structure of *L. donovani* ODC using homology modeling shows a high degree of similarity between the human

and parasite enzyme active sites, which may explain the similarity in the kinetic parameters of inhibition of the two enzymes by APA.

Experimental

Subcloning of *L. donovani* and human ODC gene fragments.

A full-length *L. donovani* ODC gene, subcloned into pET-30 Xa/LIC vector (Novagen), and a human ODC cDNA, subcloned into pUC, were amplified by PCR, using the primer pairs 5'-ATGGGTGATCATGACGTCG-3'/5'-TTATCACTCGCTCACACACCTCA-3' and 5'-ATGAACAACTTTGGTAATGAAGAGTTTG-3'/5'-TACACATTAATACTAGCCGAAGCACAG-3', respectively. PCR was performed in a 20 µl reaction volume containing 3 ng of the template, 0.5 µM each of forward and reverse primers, and 1X Phusion™ High-Fidelity PCR Master Mix (Finnzymes, Finland). The amplifications were performed in a temperature gradient DNA Thermal Cycler under the following conditions: initial denaturation (98 ºC for 30 sec), and then 29 cycles of 98 ºC for 10 sec, 48-72 ºC for 30 sec (annealing), and 72 ºC for 10 sec (extension). A final extension was carried out at 72 ºC for 10 min. The reaction mixture was further incubated with 0.8U of Taq DNA Polymerase (Fermentas, Germany) in order to introduce sticky ends for subsequent cloning into pEXP5-NT/TOPO TA vector (Invitrogen). The amplified DNA fragments were cloned into pEXP5-NT/TOPO TA vector according to the manufacturer's instructions. PCR was used to identify colonies with correctly oriented inserts, which then were sequenced. The constructs without any introduced mutations were used for transformation of BLR (DE3) chemically competent *Escherichia coli*.

Expression and purification

A single colony of transformed *E. coli* was grown overnight at 37 ºC in Luria-Bertani medium containing 100 µg/ml of ampicillin. For *L. donovani* ODC, the overnight culture was diluted 1.5:100 and incubated for 22 h at 20 ºC. The expression of *L. donovani* ODC was very high even without the addition of the inducer, isopropyl-β-D-

thiogalactopyranoside (IPTG) (leaky expression). For human ODC, the overnight culture was diluted 1.5:100 and incubated at 37 ºC until OD_{600nm} reached 0.5. The culture was then induced with 1 mM of IPTG and further incubated for four hours at 37 ºC. Bacteria cultures were harvested by centrifugation for 15 min and the pellet was stored at -80 ºC until use.

The frozen cell pellet from a 1 L culture was thawed on ice and resuspended in 10 ml lysis buffer (50 mM Tris-HCl pH 8.0, 300 mM NaCl, 1 mM DTT, 1 mM phenylmethylsulfonyl fluoride (PMSF), 0.02 % Brij 35) containing 5 mM imidazole. The lysis buffer for *L. donovani* did not contain imidazole. The cells were sonicated and the lysate centrifuged at 100,000 x g for 1 h at 4 ºC. The supernantant was mixed with 2 ml of a 50 % Ni-NTA Agarose (Qiagen) and left at 4 ºC with shaking for 2 h. The agarose was then loaded in a column. For *L. donovani* ODC the column was washed with lysis buffer containing increasing concentrations of imidazole: 8 mM (15 ml) and 20 mM (4 ml), and the $(His)_6$-tagged *L. donovani* ODC was eluted with 8 ml of buffer containing 250 mM imidazole. For human ODC, the column was washed with lysis buffer first containing 20 mM (15 ml) and then 40 mM (4 ml) imidazole, and the $(His)_6$-tagged human ODC was eluted with 8 ml of buffer containing 250 mM imidazole. The 8 ml affinity purified proteins were diluted with 42 ml of buffer A (20 mM Tris-HCl pH 8.0, 1 mM PMSF, 2 mM DTT) and passed through a Mono Q column (5/50 GL, Amersham). The proteins were eluted with a salt gradient using buffer B (20 mM Tris-HCl pH 8.0, 1 mM PMSF, 2 mM DTT, 1 M NaCl). The peaks on the chromatogram were analysed on an SDS-PAGE gel and the fractions from a single peak containing the protein of interest were concentrated and run on a gel filtration column (Superdex 200 HR 10/30) with 25 mM Hepes pH 7.2, 2 mM DTT, 0.5 mM EDTA, 0.02 % Brij 35, 1 mM PMSF with and without 0.02 mM PLP. The gel filtration fractions of each protein were concentrated to about 6 mg/ml, aliquoted and stored at -20 ºC and 4 ºC.

Kinetics analyses

Purified preparations of human and *L. donovani* ODC were used for kinetic analyses. The ODC activity was assayed at 37 ºC by measuring the release of $^{14}CO_2$ from L-[1-^{14}C] ornithine in 0.1 M Tris-HCl pH 7.5, containing 2.5 mM dithiothreitol, 0.1 mM EDTA and

0.1% Tween 80 [27]. Determination of the K_m/V_{max} for the substrate and K_d for the coenzyme was achieved by varying the concentrations of L-ornithine and PLP, respectively, in the assay.

The K_i of APA was determined by measuring its effects at various concentrations on the apparent K_m for the substrate. The kinetics of time-dependent, irreversible inhibition of ODC by DFMO was determined by incubating the enzyme with various concentrations of DFMO for different times, whereupon remaining ODC activity was measured during 5 min. The results of the kinetics analysis are shown in Table 1.

Crystallization and data collection

Attempts to crystallize the human ODC-APA complexes using the earlier reported conditions [23] did not succeed. A screen was performed in the search for new crystallization conditions. The protein solution used in the screens contained 6 mg/ml of protein (in 25 mM Hepes pH 7.2, 2 mM DTT, 0.5 mM EDTA, 0.02 % Brij 35 and 1 mM PMSF) and was pre-incubated with 2 mM APA for 10 min at room temperature before setting up crystallization drops. Initial conditions were found using the Index Screen (HR2-144, Hampton Research) by mixing equal volumes of protein and well solution in sitting drops (500 microliter well solution) at 15 °C. Needle clusters appeared after two days in 25 % PEG3350, 0.2 M ammonium acetate, 0.1 M Bis-Tris pH 6.5. Further optimization of this condition yielded fairly single crystals in 18 % PEG3350, 0.2 M ammonium acetate, 0.1 M Bis-Tris pH 6.5 and 3 mg/ml protein concentration. Data was collected to 3.0 Å at beamline I911-3, Max Lab, Lund. The crystals belonged to space group $P2_12_12_1$, with cell dimensions a=60.5, b=104.8, c=137.4, which is similar to the space group and cell constants of the crystals of the earlier structure (a=61.7, b=107.4, c=139.7, [23]). The structure was solved by molecular replacement using the coordinates of the native human ODC (PDB code 1D7K) with all water molecules removed.

For the human ODC-PLP-APA complex 6 mg/ml protein, gel-filtered in a buffer containing 0.02 mM PLP, was pre-incubated with 2 mM APA for 10 min at room temperature. Equal volumes of protein and well solution containing 25 % PEG3350, 0.2 M ammonium acetate, 0.1 M Bis-Tris pH 6.5 were mixed in sitting drops at 15 °C. Needle clusters appeared after two days. However, attempts to get single crystals from

these clusters were not successful. Subsequently, the buffer in the well solution was changed to MES, pH 6.5, and Hampton additive screens I, II and III were used in the search for possible additives which could improve the crystal quality. The crystallization buffer which yielded new large and single crystals contained 0.1 mM MES pH 6.5 and 0.3 % 1, 5-diaminopentane 2X HCl as additive (additive # 12 of Hampton additive screen 11, cadaverine). Data to 1.9 Å was collected from these crystals at beamline I911-2, MAX Lab Lund, Sweden. Only 1:1 (2 μL sitting drops over 500 μL well solution) drops gave crystals. The crystals belonged to space group C2 with cell dimensions a=108.0, b=87.1, c=130.1, β=91.0 and one dimer in the asymmetric unit.

Prior to data collection, crystals were transferred to 25 % glycerol for a few seconds before flash freezing in a boiled-off liquid nitrogen stream at 100 K. Data were processed using the XDS package [28]. The data quality was checked with the program TRUNCATE [29]. A summary of the data statistics is shown in Table 2.

Structure determination and refinement

Molecular replacement using the program PHASER [30] and the coordinates of subunit A of the native human ODC structure with solvent molecules removed (1D7K, [23]) were used in the search for two molecules per asymmetric unit. Coot [31] and refmac5 [32] were used for model building and refinement, respectively. Non-crystallographic symmetry with tight main chain and loose side chain restraints was used in the refinement of the ODC-APA complex. The library files of the ligands were generated by the PRODRG2 server [33]. Model quality was checked with PROCHECK [34] and the validation menu available in Coot [31].

Results

Kinetic analysis of ODC

Table 1 shows that the K_m value for the substrate L-ornithine was about 5-fold higher for *L. donovani* ODC than for the human enzyme. However, the k_{cat} values did not differ markedly between the two enzymes. In fact a higher value was obtained for *L. donovani* ODC compared to that of the human enzyme, which most likely only reflects minor differences in the quality of the preparations. Nevertheless, the catalytic efficiency value (k_{cat}/K_m) was still higher for the human enzyme compared to *L. donovani* ODC (Table 1). The apparent dissociation constants for the coenzyme PLP were 0.54 μM and 0.05 μM for the *L. donovani* and human ODCs, respectively (Table 1). Both enzymes were effectively inhibited *in vitro* by DFMO in a time- and concentration-dependent manner (results not shown). The inhibition followed first-order kinetics and both enzymes exhibited a 5 min half life ($T_{1/2}$) of activity at infinite DFMO concentration (Table 1). However, the apparent dissociation constant (K_d) for DFMO was 5-fold higher for *L. donovani* ODC compared to that of the human ODC (Table 1). The ODC inhibitor APA proved to be a highly potent inhibitor of *L. donovani* ODC with a K_i of 1.0 nM, which actually was somewhat lower than that found for the human enzyme (Table 1).

The structure of the human ODC-APA-PLP complex

During the refinement of the ODC-APA-PLP complex residues 1 to 6 could be built into the electron density of both subunits of the dimer. In addition, nine residues after the N-terminal methionine were built for subunit A and eight residues for subunit B. These extra residues are part of the His-tag present in the cloning vector and together they form an additional 15-residues long helix, absent in the 1D7K structure used in the molecular replacement search. Residues from this helix are involved in crystal contacts which probably explain the different space group, as compared to the 1D7K structure. The protease sensitive loop (residues 158-168, [23;35]), which in the 1D7K structure had high temperature factors (60-80 $Å^2$), has well defined density in the present model with temperature factors refined to around 20 $Å^2$. The loop also appears to adopt a different conformation, compared to that in the apo-structure and moves towards the core of the α/β-barrel, closer to the active site pocket (Figures 1A and 1B). In this position, the loop

seems to contribute to the stabilization of substrate binding. The loop next to the protease sensitive loop (residues 197-205) also moves towards the active site. However, residues 298-310 and 423-461 still could not be modeled. The final refined dimer has a total of 939 amino acid residues, which include 861 ODC residues and 17 residues from the tag. In addition, there were 2 PLP molecules, 2 APA, 2 cadaverine molecules and 3 acetate groups. The crystallographic R and R_{free} had values of 18.4 % and 21.3 %, respectively (Table 2).

PLP and APA binding

PLP and APA binding is shown in Figures 2A and 2B. A superposition of this complex with the 1D7K structure gives root-mean square deviation (rmsd) of 0.78 Å involving 3128 atoms. The present complex shows that PLP binds in a position similar to that reported earlier for mouse and *T. brucei* ODC [20;21], with some differences in the binding mode (Figure 2A). Thus, the Shiff base link to the co-factor from Lys^{69} is absent. Unlike the mouse ODC structure, the Nζ group of the invariant Lys^{69} is turned away from O4, making a hydrogen bond to the side chain of Asp^{88} and two solvent molecules. The O4 group of PLP is rotated and is hydrogen bonded with the 1-aminooxy group of the inhibitor, APA. Nε2 of His^{197} makes a hydrogen bond with OP4 of PLP, and OP1 makes a water-mediated hydrogen bond with Nε of Arg^{277}. In contrast, in the complex of mouse ODC with PLP there is a direct interaction between OP1 and Arg^{277}. The pyridine nitrogen N1 interacts with Asp^{274}, in a similar manner to the mouse structure, while the distance to the side chain of Asp^{88} is slightly shorter (3.1 Å and 3.7 Å for the human and mouse structure, respectively). The side chain of Cys^{360} is rotated by about 180° towards the bound inhibitor, occupying a position of 3.7 Å from the oxygen of the hydroxylamine moiety of APA.

The efficiency and specificity of hydroxylamine-containing inhibitors of PLP- or pyruvate-dependent enzymes has been attributed to the properly positioned functional groups in the alkyl fragment, securing structural similarity with the substrate or product of the enzymatic reaction [19;21;36]. In the present complex APA essentially occupies the position of the substrate in the active site (Figure 2B and 2C), with only some slight differences in the positions of the atoms. Its positively charged 3-amino group, previously

suggested to anchor the molecule to the enzyme [19], interacts with Oδ1 of Asp^{332}, the backbone carbonyl of Tyr^{331} (from subunit A) and a solvent molecule. This solvent molecule in turn makes hydrogen bonds to Asp^{361} and Tyr^{323} (from subunit B). The complex also shows that all the other residues earlier reported to be involved in substrate binding through hydrogen bonding or hydrophobic interactions, are also involved in APA binding [21;22;37;38]. As mentioned above, the 1-aminooxy moiety of APA is at a hydrogen bonding distance from O4 of PLP. In the A subunit this distance is around 3.0 Å, somewhat longer than the corresponding distance in the B subunit, which is 2.7 Å. The B subunit binding site has also a contribution from the side chain of Cys^{164} which makes a water mediated hydrogen bond to the 3-amino group of APA. The methylene groups of APA are involved in hydrophobic interactions with Tyr^{389} (subunit A) and Tyr^{323} (subunit B). Some residues from the protease sensitive loop lie within 5 Å from APA. There are also 3 crystallographic waters in the binding site of each subunit. (Figure 2C). This is in contrast to the complex of *T. brucei* ODC with DFMO, which had six water molecules [21]. In the present complex these water molecules are displaced by the protease-sensitive loop, which was, as mentioned above, disordered in the *T. brucei* DFMO complex. The new position of the loop also results in a closer fit of APA to the binding pocket, which would add to its high affinity. This could be contrary to the hydroxylamine-derived inhibitors of mitochondrial aspartate aminotransferase whose binding has been proposed to be driven by the high reactivity of the aminooxy moiety, rather than by high degree of complementarity to the binding site [19].

Interestingly, in the absence of PLP, APA binds at approximately 7 Å from its position in the complex with PLP, and it partially occupies the site of the PO4 group of PLP (Figure 3). However, this binding has probably no physiological relevance.

Cadaverine binding site

Cadaverine, which was used as an additive in the crystallization, was bound with an extended conformation inside a surface-exposed pocket between the N- and C-terminal domains of the molecule in close vicinity to the active site (Figure 4). In subunit A of the protein the 1-amino group forms water-mediated hydrogen bonds with the backbone carbonyl groups of Gly^{237} and Cys^{202}, while the 5-amino group makes a bond to the side

chain of Ser^{241}. Other potential interactions within a radius of 3.5 Å to 4 Å involve Gly^{201}, Val^{244}, Pro^{239}, Leu^{246}, Arg^{277} and Asn^{385}. It is also seen from the figure that some residues from the protease sensitive loop are within approximately 5 Å from cadaverine. The closest distance to APA and PLP is 10 Å and 7.3 Å, respectively, which is rather high for any direct interaction to take place. On the other hand the closest distance to Arg^{277}, which is crucial for ODC activity, is only 3.5 Å. Although cadaverine binding in this structure is most probably unspecific, the presence of an invariant residue in combination with some variable residues within the binding pocket may be used in the design of new species-specific inhibitors of ODC. The unspecific binding of cadaverine in this structure is illustrated by the fact that its position in subunit B is slightly different. It is closer to the surface of the molecule and has a much smaller number of interactions with the protein.

Discussion

L. donovani has earlier been cloned [39], and its kinetic parameters were subsequently analyzed together with those of the mouse and *T. brucei* enzymes [40;41]. The K_m and k_{cat} reported here for *L. donovani* ODC are similar to the values reported earlier by Osterman et al. [40]. Also the K_m value for the human ODC is similar to that reported for the mouse enzyme, while k_{cat} is somewhat lower [40]. Our results clearly confirm that *L. donovani* ODC has kinetic properties that are distinct from those of the human ODC. Thus, the binding affinity for L-ornithine and PLP are 5- and 11-fold lower, respectively, for *L. donovani* compared to the human enzyme. In addition, the apparent dissociation constant (K_d) for DFMO was 5-fold higher for *L. donovani*. Since DFMO binding mimics substrate binding to ODC, the difference in K_d is in good agreement with the observed difference in affinity for L-ornithine. These results, together with the observation that *L. donovani* ODC was not able to form cross-species heterodimers with the *T. brucei* and mouse enzymes, [40], indicate that *L. donovani* ODC has a potential of being targeted for drug development against leishmaniasis.

The present study shows that *L. donovani* and human ODC are strongly inhibited by APA, with Ki values around 1.0 nM. Comparable results were reported for the mouse and *P. falciparum* ODC, which had Ki values of 3.2 nM and 3 nM, respectively [13;15]. Recent results also show that treatment with APA and its derivatives reduces the

intracellular polyamine concentrations, with a concomitant antiproliferative effect in cultured cancer cells [15]. It also shows clear anti-parasitic effect in *P. falciparum* and *L. donovani* cells [13;15;17].

The first step in the reaction mechanism of ODC is expected to be the formation of a Schiff base between L-ornithine and PLP, and the loss of the bond between Lys^{69} and PLP [42]. The aminooxy group of APA is unprotonated at physiological pH and is believed to form an oxime with PLP [18], which would mimic the Schiff base formed between the substrate and PLP [22;36;37;43;44]. The structure of the complex between APA and human ODC clearly shows that APA competes with L-ornithine for the substrate binding site, although the Lys^{69}-PLP Schiff base link is broken and no oxime was formed between APA and PLP. APA is also bound in a bent conformation, with its aminooxy group pointing away from PLP. One possible explanation for the absence of the oxime formation could be the presence of Cadaverine in close vicinity to the active site. Cadaverine may affect the position of PLP, which appears to be slightly different in the present complex, as compared to the mouse ODC-PLP complex. It should be noted that the cadaverine binding site found between the two domains in this work is different from the site occupied by geneticin in complex with *T. brucei* ODC. Geneticin (Ki 5-8 mM) used at a concentration of 200 mM in the crystallization, was able to sufficiently inhibit the slow decarboxylation of D-ornithine by ODC, allowing the observation of D-ornithine bound in the active site [39].

Further understanding of the sequences of human and *L. donovani* enzymes as well as the role of the N-terminal extension in *L. donovani* ODC may help in future development of new drugs against leishmaniasis.

Acknowledgments

This work was supported by a grant from the Research School in Pharmaceutical Sciences at Lund University (FLÄK) to SAK, SIDA-SAREC grant from the Swedish International Development Cooperation Agency, and grants from the Swedish Research Council, the J. C. Kempe Memorial Foundation, the Royal Physiographic Society in Lund.

Reference List

1 Pegg,A.E. (1986) Recent advances in the biochemistry of polyamines in eukaryotes. Biochem.J. **234,** 249-262.

2 Pegg,A.E. (1988) Polyamine metabolism and its importance in neoplastic growth and a target for chemotherapy. Cancer Res. **48,** 759-774.

3 Heby,O. (1981) Role of polyamines in the control of cell proliferation and differentiation.Differentiation **19,** 1-20.

4 Heby,O., Roberts,S.C. and Ullman,B. (2003) Polyamine biosynthetic enzymes as drug targets in parasitic protozoa. Biochem.Soc.Trans. **31,** 415-419.

5 Muller,S., Wittich,R.M. and Walter,R.D. (1988) The polyamine metabolism of filarial worms as chemotherapeutic target. Adv.Exp.Med.Biol. **250,** 737-743.

6 Muller,S., Coombs,G.H. and Walter,R.D. (2001) Targeting polyamines of parasitic protozoa in chemotherapy. Trends in Parasitology **17,** 242-249.

7 Phillips,M.A. and Wang,C.C. (1987) A Trypanosoma brucei mutant resistant to alpha-difluoromethylornithine. Mol.Biochem.Parasitol. **22,** 9-17.

8 Bitonti,A.J., McCann,P.P. and Sjoerdsma,A. (1987) Plasmodium falciparum and Plasmodium berghei: effects of ornithine decarboxylase inhibitors on erythrocytic schizogony. Exp.Parasitol. **64,** 237-243.

9 Kaur,K., Emmett,K., McCann,P.P., Sjoerdsma,A. and Ullman,B. (1986) Effects of DL-alpha-difluoromethylornithine on Leishmania donovani promastigotes. J.Protozool. **33,** 518-521.

10 Khomutov,R.M., Hyvonen,T., Karvonen,E., Kauppinen,L., Paalanen,T., Paulin,L., Eloranta,T., Pajula,R.L., Andersson,L.C. and Poso,H. (1985) 1-Aminooxy-3-aminopropane, a new and potent inhibitor of polyamine biosynthesis that inhibits

ornithine decarboxylase, adenosylmethionine decarboxylase and spermidine synthase. Biochem.Biophys.Res.Commun. **130,** 596-602.

11 Seiler,N. (2003) Thirty years of polyamine-related approaches to cancer therapy. Retrospect and prospect. Part 1. Selective enzyme inhibitors. Curr.Drug Targets. **4,** 537-564.

12 Das,G.R., Krause-Ihle,T., Bergmann,B., Muller,I.B., Khomutov,A.R., Muller,S., Walter,R.D. and Luersen,K. (2005) 3-Aminooxy-1-aminopropane and derivatives have an antiproliferative effect on cultured Plasmodium falciparum by decreasing intracellular polyamine concentrations. Antimicrob.Agents Chemother., **49,** 2857-2864.

13 Hyvonen,T., Alakuijala,L., Andersson,L., Khomutov,A.R., Khomutov,R.M. and Eloranta,T.O. (1988) 1-Aminooxy-3-aminopropane reversibly prevents the proliferation of cultured baby hamster kidney cells by interfering with polyamine synthesis. J.Biol.Chem. **263,** 11138-11144.

14 Mett,H., Stanek,J., Lopez-Ballester,J.A., Janne,J., Alhonen,L., Sinervirta,R., Frei,J. and Regenass,U. (1993) Pharmacological properties of the ornithine decarboxylase inhibitor 3-aminooxy-1-propanamine and several structural analogues. Cancer Chemother.Pharmacol. **32,** 39-45.

15 Milovica,V., Turchanow,l., Khomutov,A.R., Khomutov,R.M., Caspary,W.F. and Stein,J. (2001) Hydroxylamine-containing inhibitors of polyamine biosynthesis and impairment of colon cancer cell growth. Biochem.Pharmacol, **61,** 199-206.

16 Singh,S., Mukherjee,A., Khomutov,A.R., Persson,L., Heby,O., Chatterjee,M. and Madhubala,R. (2007) Antileishmanial effect of 3-aminooxy-1-aminopropane is due to polyamine depletion. Antimicrob.Agents Chemother. **51**(2):528-34

17 Stanek,J., Frei,J., Mett,H., Schneider,P. and Regenass,U. (1992) 2-substituted 3-(aminooxy)propanamines as inhibitors of ornithine decarboxylase: synthesis and biological activity. J.Med.Chem. **35,** 1339-1344.

18 Khomutov,A.R. (2002) Inhibition of enzymes of polyamine biosynthesis by substrate-like O-substituted hydroxylamines. Biochemistry (Mosc.) **67,** 1159-1167.

19 Markovic-Housley,Z., Schirmer,T., Hohenester,E., Khomutov,A.R., Khomutov,R.M., Karpeisky,M.Y., Sandmeier,E., Christen,P. and Jansonius,J.N. (1996) Crystal structures and solution studies of oxime adducts of mitochondrial aspartate aminotransferase. Eur.J.Biochem. **236,** 1025-1032.

20 Kern,A.D., Oliveira,M.A., Coffino,P. and Hackert,M.L. (1999) Structure of mammalian ornithine decarboxylase at 1.6 A resolution: stereochemical implications of PLP-dependent amino acid decarboxylases. Structure.Fold.Des. **7,** 567-581.

21 Grishin,N.V., Osterman,A.L., Brooks,H.B., Phillips,M.A. and Goldsmith,E.J. (1999) X-ray structure of ornithine decarboxylase from Trypanosoma brucei: the native structure and the structure in complex with alpha-difluoromethylornithine. Biochemistry **38,** 15174-15184.

22 Jackson,L.K., Brooks,H.B., Osterman,A.L., Goldsmith,E.J. and Phillips,M.A. (2000) Altering the reaction specificity of eukaryotic ornithine decarboxylase. Biochemistry **39,** 11247-11257.

23 Almrud,J.J., Oliveira,M.A., Kern,A.D., Grishin,N.V., Phillips,M.A. and Hackert,M.L. (2000) Crystal structure of human ornithine decarboxylase at 2.1 A resolution: structural insights to antizyme binding. J.Mol.Biol. **295,** 7-16.

24 Coleman,C.S., Stanley,B.A., Viswanath,R. and Pegg,A.E. (1994) Rapid exchange of subunits of mammalian ornithine decarboxylase. J.Biol.Chem. **269,** 3155-3158.

25 Tobias,K.E. and Kahana,C. (1993) Intersubunit location of the active site of mammalian ornithine decarboxylase as determined by hybridization of site-directed mutants. Biochemistry **32,** 5842-5847.

26 Osterman,A.L., Brooks,H.B., Rizo,J. and Phillips,M.A. (1997) Role of Arg-277 in the binding of pyridoxal 5'-phosphate to Trypanosoma brucei ornithine decarboxylase. Biochemistry **36,** 4558-4567.

27 Janne,J. and Williams-Ashman,H.G. (1970) Mammalian ornithine decarboxylase: activation and alteration of physical behaviour by thiol compounds. Biochem.J. **119,** 595-597.

28 French,G.S. and Wilson,K.S. (1978) On the treatment of negative intensity observations. Acta Cryst. **A34**, 517-525.

29 Storoni,L.C., McCoy,A.J. and Read,R.J. (2004) Likelihood-enhanced fast rotation functions. Acta Crystallogr.D.Biol.Crystallogr. **60,** 432-438.

30 McCoy,A.J., Grosse-Kunstleve,R.W., Storoni,L.C. and Read,R.J. (2005) Likelihood-enhanced fast translation functions. Acta Crystallogr.D.Biol.Crystallogr. **61,** 458-464.

31 Emsley,P. and Cowtan,K. (2004) Coot: model-building tools for molecular graphics. Acta Crystallogr.D.Biol.Crystallogr. **60,** 2126-2132.

32 Murshudov,G.N., Vagin,A.A. and Dodson,E.J. (1997) Refinement of macromolecular structures by the maximum-likelihood method. Acta Crystallogr.D.Biol.Crystallogr. **53,** 240-255.

33 Schuttelkopf,A.W. and van Aalten,D.M. (2004) PRODRG: a tool for high-throughput crystallography of protein-ligand complexes. Acta Crystallogr.D.Biol.Crystallogr. **60,** 1355-1363.

34 Laskowski,R.A., MacArthur,M.W., Moss,D.S. and Thorton,J.M. (1993) PROCHECK: a program to check the sterochemical quality of protein structures. J.Appl.Cryst. **26,** 283-291.

35 Osterman,A.L., Lueder,D.V., Quick,M., Myers,D., Canagarajah,B.J. and Phillips,M.A. (1995) Domain organization and a protease-sensitive loop in eukaryotic ornithine decarboxylase. Biochemistry **34,** 13431-13436.

36 Shah,S.A., Shen,B.W. and Brunger,A.T. (1997) Human ornithine aminotransferase complexed with L-canaline and gabaculine: structural basis for substrate recognition. Structure. **5,** 1067-1075.

37 Jackson,L.K., Goldsmith,E.J. and Phillips,M.A. (2003) X-ray structure determination of Trypanosoma brucei ornithine decarboxylase bound to D-ornithine and to G418: insights into substrate binding and ODC conformational flexibility. J.Biol.Chem. **278,** 22037-22043.

38 Jackson,L.K., Brooks,H.B., Myers,D.P. and Phillips,M.A. (2003) Ornithine decarboxylase promotes catalysis by binding the carboxylate in a buried pocket containing phenylalanine 397. Biochemistry **42,** 2933-2940.

39 Hanson,S., Adelman,J. and Ullman,B. (1992) Amplification and molecular cloning of the ornithine decarboxylase gene of Leishmania donovani. J.Biol.Chem. **267,** 2350-2359.

40 Osterman,A., Grishin,N.V., Kinch,L.N. and Phillips,M.A. (1994) Formation of functional cross-species heterodimers of ornithine decarboxylase. Biochemistry **33,** 13662-13667.

41 Osterman,A.L., Kinch,L.N., Grishin,N.V. and Phillips,M.A. (1995) Acidic residues important for substrate binding and cofactor reactivity in eukaryotic ornithine decarboxylase identified by alanine scanning mutagenesis. J.Biol.Chem. **270,** 11797-11802.

42 Brooks,H.B. and Phillips,M.A. (1997) Characterization of the reaction mechanism for Trypanosoma brucei ornithine decarboxylase by multiwavelength stopped-flow spectroscopy. Biochemistry **36,** 15147-15155.

43 Burkhard,P., Tai,C.H., Jansonius,J.N. and Cook,P.F. (2000) Identification of an allosteric anion-binding site on O-acetylserine sulfhydrylase: structure of the enzyme with chloride bound. J.Mol.Biol. **303,** 279-286.

44 Gokulan,K., Rupp,B., Pavelka,M.S., Jr., Jacobs,W.R., Jr. and Sacchettini,J.C. (2003) Crystal structure of Mycobacterium tuberculosis diaminopimelate decarboxylase, an essential enzyme in bacterial lysine biosynthesis. J.Biol.Chem. **278,** 18588-18596.

45 DeLano,W.L. (2002) The PyMOL Molecular Graphics System. DeLano Scientific, San Carlos, CA, USA.

46 Wallace,A.C., Laskowski,R.A. and Thornton,J.M. (1995) LIGPLOT: A program to generate schematic diagrams of protein-ligand interactions. Prot.Eng. **8,** 127-134.

47 Diederichs,K. and Karplus,P.A. (1997) Improved R-factors for diffraction data analysis in macromolecular crystallography. Nat.Struct.Biol. **4,** 269-275.

Figure 1. (A) A ribbon model showing a stereo view of the superposition of the human apo-ODC (PDB id 1D7K, shown in green) and human ODC-PLP-APA complex (orange and blue for subunits A and B, respectively). The two conformations of the protease sensitive loop (residues 158-168) are shown in grey for the apo-structure and magenta for the ODC-PLP-APA complex.
(B) A close up stereo view showing the two conformations of the protease sensitive loop, APA, PLP and cadaverine (Cad). The coloring of the protease-sensitive loop is as in Figure 1A. APA, PLP, and cadaverine are shown as sticks (yellow, blue and red for carbon, nitrogen, and oxygen, respectively). All structural figures were generated with Pymol [45].

Figure 2. (A) Superposition of the structure of mouse ODC (PDB id 7ODC, green) and human ODC-PLP-APA complex (light blue) showing O4 of PLP flipped towards APA, thus breaking the Schiff-bond to Lys^{69}. Lys^{69} is turned towards Asp^{88}. PLP, APA and amino acid side chains are shown as sticks, coloring as in Figure 1.
(B) APA binding in the human ODC-PLP-APA complex. Subunit A is colored light blue and subunit B orange. Residues from each subunit contributing to APA binding are colored accordingly. Fo-Fc electron density map contoured at 3 σ is shown covering APA. This density was calculated with APA omitted. Side chains of amino acid residues are shown as sticks. Solvent molecules are shown as orange spheres.
(C) A schematic diagram showing the interactions of APA with neighboring groups within the active site. Water molecules are light blue, nitrogen, carbon and oxygen are shown in dark blue, black and red, respectively. PLP phosphorus group is shown in magenta. Numbers on the dashed lines show the distances between the atoms. Figure was generated with Ligplot [46].

Figure 3. A stereo view showing the position APA in the complex with ODC without PLP present. Fo-Fc electron density map contoured at 3 σ is shown covering APA. For comparison, PLP from the ODC-PLP-APA complex (grey) is shown superimposed on this structure. APA and PLP are shown in sticks representation.

Figure 4. A stereo view showing the cadaverine (Cad) molecule bound in a pocket between the N- and C-terminal domains (orange and blue, respectively). Fo-Fc electron density map contoured at 3 σ is shown around cadaverine. This density was calculated with cadaverine omitted. APA and PLP are shown as orange sticks. The protease sensitive loop is shown in magenta. Hydrogen bonds between cadaverine, amino acid residues or water (orange spheres) are shown as dashes in black.

Table 1. Kinetic analysis of *L. donovani* and human ODCs

ODC	K_m (mM)	k_{cat} (s^{-1})	k_{cat}/K_m (mM^{-1} s^{-1})	PLP K_d (μM)	DFMO $t_{½}$ (min)	DFMO K_d (μM)	APA K_i (nM)
L. donovani	0.39	8.1	20.8	0.54	4.8	50	1.0
Human	0.08	3.3	41.3	0.05	5.0	10	1.4

Table 2 : Data collection and refinement statistics

	ODC-PLP-APA	ODC-APA
Data collection:	MAX lab I911-2	MAX lab I911-3
Cell, a, b, c (Å) β (°)	C2, 108.02, 87.11, 130.08 91.02	$P2_12_12_1$, 60.54, 104.84, 137.35
Resolution range (Å)	30.0 –1.9	20.0 – 3.0
Completeness (%)*	99.7 (98.4)	99.6 (100)
Unique reflections	94671	18056
Multiplicity	4.8	7.2
I/σ(I)	16.84 (3.2)	12.37 (7.32)
R_{mrgd-F} (%)†	10.3 (46.8)	9.0 (13.3)
Refinement:		
No. of protein atoms	6617	6454
No. of water molecules	527	
PLP	2	
APA	2	2
Cadaverine	2	
Acetates	3	
R_{cryst} (R_{free})‡	0.184 (0.213)	0.235 (0.30)
Average B-factors (Å^2)	24.6	31.7
Rmsd from ideality		
bond lenghts (Å)	0.01	0.015
bond angles (°)	1.2	1.65
chiral (°)	0.08	0.108
Ramachandran		
Core (%)	92.3	83.1
Allowed (%)	7.7	16.6
Disallowed (%)	0	0.3

*The numbers in parentheses are for the highest resolution shell

†$R_{mrgd\text{-}F}$ as defined by [47] is a quality measure of the reduced structure factor amplitudes.

‡$R_{cryst}=\Sigma |F_{obs} - F_{calc}| / \Sigma F_{obs}$, where F_{obs} and F_{calc} are the observed and calculated structure factor amplitudes, respectively.

R_{free} is the same as R_{cryst} , but calculated on 5% of the data excluded from refinement.

Biochemical Journal Immediate Publication. Published on 4 Apr 2007 as manuscript BJ20070188

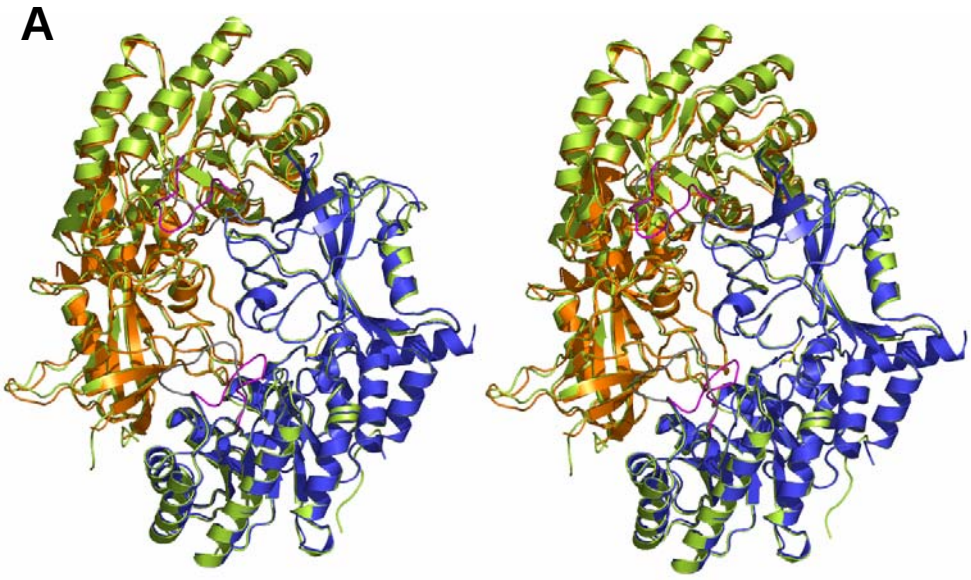

Fig. 1A

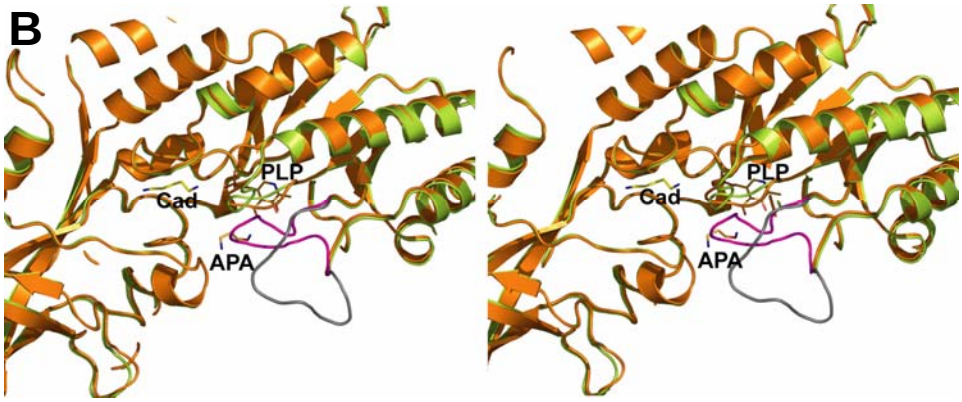

Fig. 1B

Biochemical Journal Immediate Publication. Published on 4 Apr 2007 as manuscript BJ20070188

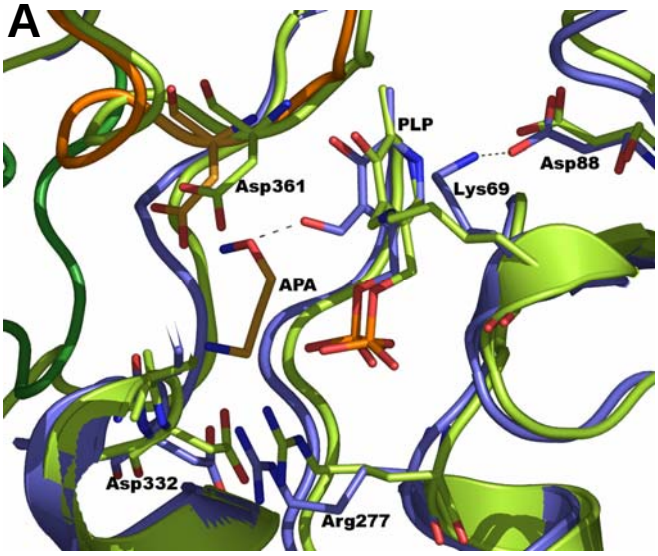

Fig. 2A

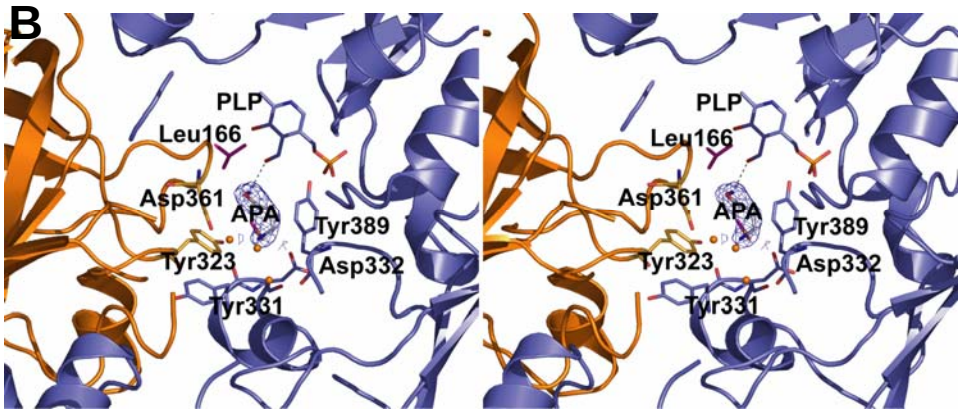

Fig. 2B

Biochemical Journal Immediate Publication. Published on 4 Apr 2007 as manuscript BJ20070188

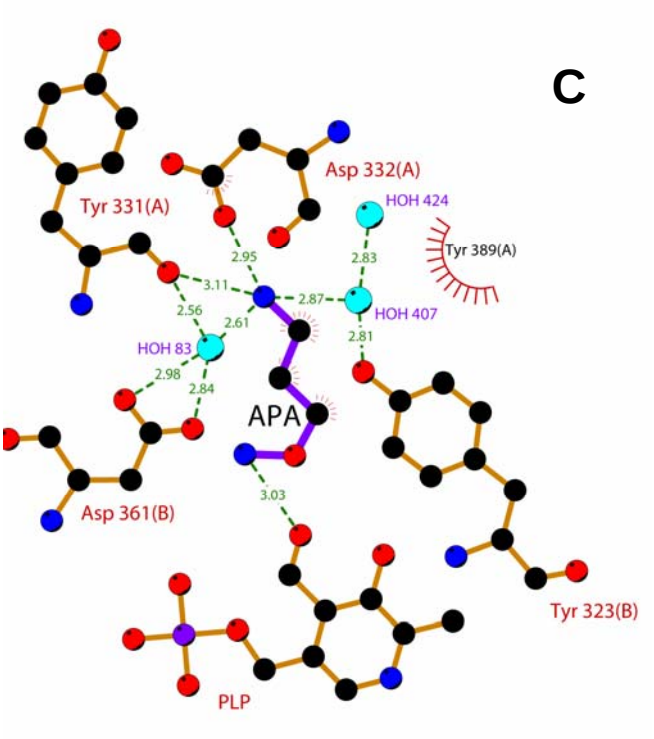

Fig. 2C

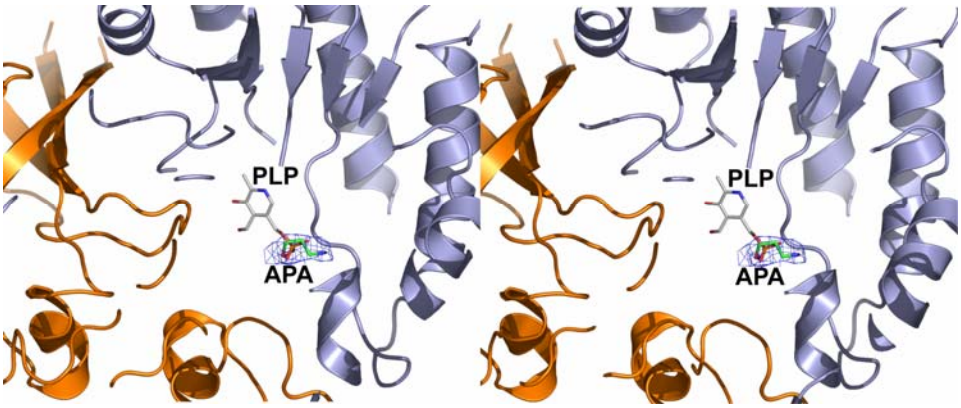

Fig. 3

Biochemical Journal Immediate Publication. Published on 4 Apr 2007 as manuscript BJ20070188

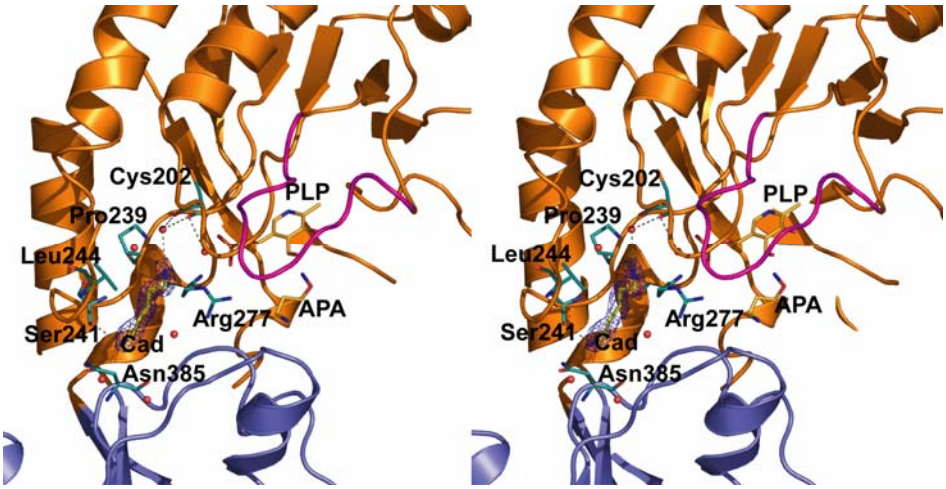

Fig. 4